Appl Phys B (2011) 104:931–934
DOI 10.1007/s00340-011-4664-3

Applied Physics B
Lasers and Optics

Integrated optical attenuator based on mechanical deformation of an elastomer layer

N. Galler · H. Ditlbacher · A. Hohenau · A. Leitner · F.R. Aussenegg · J.R. Krenn

Received: 16 June 2011 / Published online: 29 July 2011

Abstract We propose an optical attenuator concept based on a polymer waveguide coupled to an elastomer thin film. The thickness of the elastomer layer can be controlled by Coulomb force-induced squeezing in a capacitor geometry. Thereby resonant coupling between the light modes in the waveguide and the elastomer layer is achieved. We predict close to 100% modulation contrast and about 40% transmission for an about 200 μm long device. In addition, we demonstrate experimentally a proof-of-principle of the attenuator device.

1 Introduction

Besides the further development of state-of-the-art optical telecommunication devices with bandwidths in the GHz range there is an interest in small-footprint and cheap optical components addressing bandwidths in the kHz range for, e.g., protection switching and optical routing. In this context polymer materials are thoroughly investigated as they offer mechanical flexibility, potentially cheap fabrication schemes and easy integration with organic optoelectronics. In particular, elastomers that can be mechanically squeezed to achieve optical functionality have been used for realizing an optical attenuator already decades ago [1]. More recently, besides further attenuator concepts [2], a spatial light modulator [3], a phase retarder [4] and tunable diffraction gratings [5] have been demonstrated. The squeezing dynamics of an elastomer layer has been investigated in detail both experimentally [6] and theoretically [7]. In this letter, we report on an elastomer-based electromechanically actuated optical waveguide attenuator. The concept is realized as a polymer stripe waveguide sandwiched between substrate and cladding slabs. The cladding material is an elastomer that is locally squeezed due to Coulomb forces between two electrodes. A laterally structured metal thin film electrode on the stripe waveguide and a counter electrode on the cladding layer form a capacitor, as sketched in Fig. 1a [8]. Light injected into the polymer waveguide propagates towards the metal electrode that is some tens of μm long. There, due to the presence of the metal the effective index of the light mode in the polymer waveguide is reduced below the refractive index of the elastomer cladding. Consequently, leakage of light to cladding modes occurs, however, at a moderate rate so that the waveguide output intensity I_{out} is just slightly reduced (Fig. 1b). The situation is different when the mode index of the polymer waveguide mode meets the value of a cladding mode, making coupling of light from the waveguide to the cladding efficient and strongly reducing I_{out} (Fig. 1c). For properly chosen device parameters this can be managed by applying a voltage to the electrodes. The attractive electrostatic force between the electrodes leads to a reduction in thickness of the elastomer cladding in the region between the two electrodes, lowering the cladding mode index to the very value of the polymer mode.

The device as sketched in Fig. 1a is fabricated as follows. Starting point is a cleaned glass substrate spin coated with a 2.70 μm thick polytetrafluorethylene film (PTFE, $n = 1.343$). All refractive indices were measured by ellipsometry for a light wavelength of 633 nm as used in the experiment discussed below. Next, a 0.35 μm thick SU8 film ($n = 1.572$) is deposited by spin coating and electron beam lithography (EBL) is applied to shape a 3.56 μm wide stripe waveguide. Another EBL step defines the bottom electrode

N. Galler · H. Ditlbacher · A. Hohenau · A. Leitner · F.R. Aussenegg · J.R. Krenn (✉)
Institute of Physics and Erwin Schrödinger Institute for Nanoscale Research, Karl-Franzens-University, 8010 Graz, Austria
e-mail: joachim.krenn@uni-graz.at

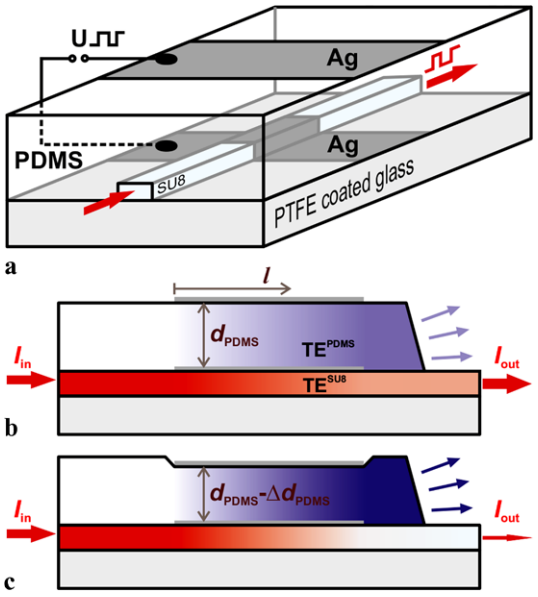

Fig. 1 Integrated optical attenuator. (**a**) Sketch of device architecture, U is the voltage applied to the electrodes for squeezing the PDMS layer. (**b**) Without an applied voltage only weak leakage from the SU8 waveguide to the PDMS cladding attenuates the output intensity I_{out}, while (**c**) efficient coupling to the electrostatically squeezed PDMS cladding and thus strongly attenuated I_{out} occurs when a voltage is applied

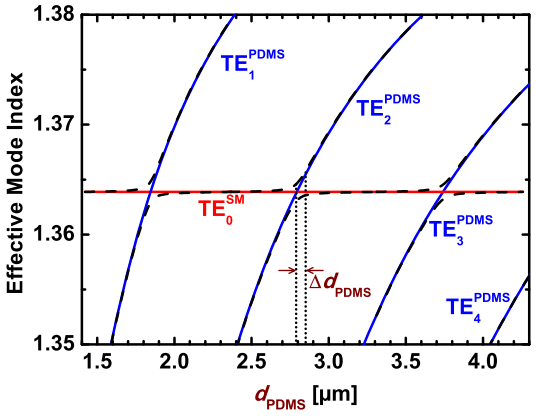

Fig. 2 The effective mode indices of the TE cladding modes as a function of the thickness of the PDMS layer, together with the mode index of the TE_0^{SM} waveguide mode. The *full and dashed lines* show the unperturbed and coupled modes, respectively. Δd_{PDMS} corresponds to the experimentally achieved thickness variation

which is a 40 nm thick silver film extending over 57 μm along the stripe waveguide axis. As the cladding a polydimethylsiloxane (PDMS, a mixture of the Dow Corning products Sylgard 184 and Sylgard 527 in volume ratio of 1:13, $n = 1.404$) layer with a thickness of 2.85 μm is deposited and a 40 nm thick silver electrode is evaporated through a shadow mask as the top electrode. Plasma treatment of the PDMS surface avoids the diffusion of silver into the layer during evaporation. We note that the thickness change of the PDMS layer is not accompanied by a refractive index change as the elastomer is incompressible with a Poisson ratio close to 0.5.

2 Theoretical modeling

We first turn to a theoretical analysis and simulation of the device. By applying the effective index method [9] we find that for a light wavelength of 633 nm the SU8 waveguide is single-mode in the direction perpendicular to the substrate plane and supports five modes in the parallel direction. While the mode indices of the two highest-order modes are lower than the refractive index of PDMS (a condition for leaking to and coupling with cladding modes) only the TE_{04}^{SU8} mode has the field symmetry to allow for efficient coupling to cladding modes. To keep the further analysis simple we use the transfer matrix method [10] to calculate the coupling of this TE_{04}^{SU8} mode with the cladding modes. Thereby we have to replace the SU8 waveguide by a slab with the same height. By assigning a hypothetical refractive index to the slab material (SM) we make sure that the mode index of the slab mode TE_0^{SM} is identical to that of the TE_{04}^{SU8} mode.

Figure 2 shows the calculated dependence of the effective mode indices of various cladding modes on the thickness of the PDMS layer, analyzed for the region including the silver electrodes. It is reasonable to assume that the TE modes guided in the SU8 waveguide are not sensitive to the thickness of the PDMS layer. We find that the TE_0^{SM} mode can couple to the PDMS modes, which is reflected in an anticrossing behavior at specific thicknesses of the PDMS layer. Due to the cladding thickness of 2.85 μm the waveguide mode is expected to couple to the TE_2^{PDMS} mode. The thickness range defined in Fig. 2 as Δd_{PDMS} corresponds to the experimental value discussed below.

In Fig. 3 the calculated respective intensities of the waveguide mode TE_0^{SM} and the cladding mode TE_2^{PDMS} are plotted versus the propagation coordinate l, which is set to 0 at the onset of the silver electrode. For $l = 0$ the whole intensity is guided by definition in the TE_0^{SM} mode. By propagating further along l the intensity is transferred to the TE_2^{PDMS} mode and finally the mode intensities oscillate between the SU8 and PDMS layers which form a directional coupler. We point out that for rather high values of l our model assumptions are expected to fail to properly describe the actual device as the lateral spread of light coupled to the PDMS layer from the 3.56 μm wide SU8 stripe waveguide is not considered. The intensities as plotted in Fig. 3 are enveloped by an exponential decay due to losses in the metal layers. The full and the dashed lines show the results for 2.85 and 2.79 μm thick PDMS layers, respectively, which reflect the experimentally achieved thickness variation. Importantly, for an

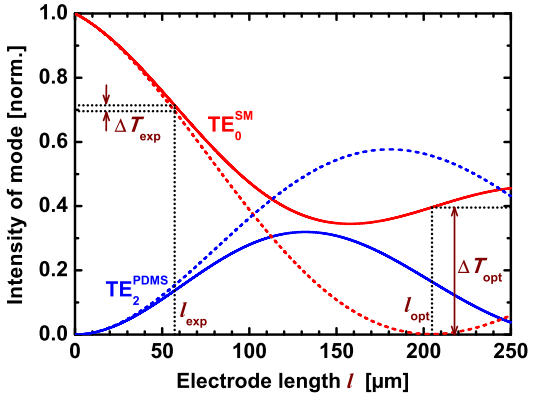

Fig. 3 The intensities of the TE_0^{SM} and TE_2^{PDMS} modes plotted versus the propagation coordinate l which is set to 0 at the onset of the silver electrode. The *full and dashed lines* give the calculated values for a PDMS thickness of 2.85 and 2.79 µm, respectively. l_{exp} and l_{opt} denote the respective experimentally used and optimum electrode length, ΔT_{exp} and ΔT_{opt} the according values of light transmission modulation

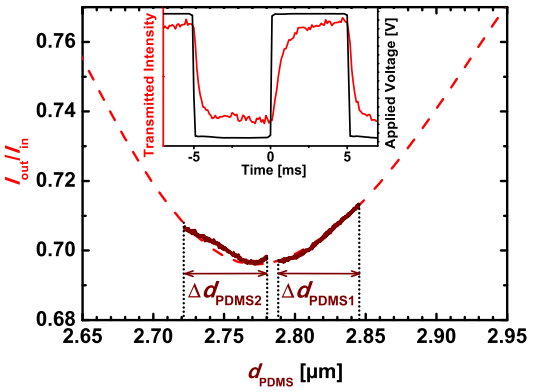

Fig. 4 Measured optical transmission through the SU8 waveguide as a function of the thickness of the PDMS layer (*full lines*) combined with the calculated curve (*dashed line*). Δd_{PDMS1} and Δd_{PDMS2} mark the PDMS thickness variations achieved for two different samples. The inset depicts the temporal response of the device

electrode length of 206 µm the simulation predicts a modulation amplitude of 100% at a maximum transmission of about 40%. This we consider an important result emphasizing that relevant device performance can be achieved over extremely short propagation lengths.

3 Experimental

We now demonstrate a proof-of-principle of the device outlined above. For the waveguide transmission measurements light from a helium neon laser (wavelength 633 nm) is injected into a monomode fiber and butt-coupled to the cleaved SU8 waveguide. By varying the lateral position of the fiber end with respect to the waveguide input the TE_{04}^{SU8} mode can be excited with high selectivity as we deduce from the good agreement of the measured change in waveguide transmission with the respective calculated values (see below). At the output side of the device the PDMS cladding is removed over a length of a few millimeters to ensure the separation of light guided in the SU8 stripe and the PDMS cladding, as schematically shown in Figs. 1b, 1c).

The output of the SU8 waveguide is imaged onto a photodiode using a microscope objective (40x, numerical aperture = 0.65). By applying a voltage ramp (0 to 150 V) to the electrodes the thickness of the PDMS layer changes in proportion with the square of the voltage, as deduced from measuring the Fabry–Pérot modes within the PDMS layer in the direction perpendicular to the interfaces in the waveguide system [6]. The measured optical transmission for a thickness variation from 2.85 µm to 2.79 µm is plotted in Fig. 4 by the full line labeled Δd_{PDMS1}. To enlarge the accessible PDMS thickness range for comparison with the simulations we have fabricated a second sample with a PDMS thickness of 2.78 µm which can be compressed to a thickness of 2.72 µm, leading to the variation of the transmitted light labeled Δd_{PDMS2}. When comparing these experimental data with the calculated dependence of the waveguide transmission on the PDMS thickness as plotted by the dashed line we find an excellent agreement (Fig. 4). In particular, the transmission dip is well reproduced by the measurements indicating that indeed mode coupling leads to the observed transmission dependence. The change in transmission is about 2% which is the very value that we find from the model calculations (Fig. 3, at $l = 57$ µm). The inset shows the temporal response of the device, indicating a switching time (0 to 90% of the modulation amplitude) of around 1 ms.

4 Conclusions

Clearly the experimentally observed transmission modulation of 2% falls short of the simulated potential of our device. We identify as the main reason for this discrepancy that in our experiment the PDMS modes are not guided laterally, i.e. they diverge during propagation, which is not covered by the model. The influence of this divergence on modulator operation increases with the electrode length so that we were unable to retrieve meaningful signals for electrode lengths of more than 100 µm. To avoid this divergence the PDMS layer should be structured in a stripe geometry, in analogy to the SU8 waveguide. Preliminary results show that therefore both reactive ion etching and focused ion beam milling are feasible, a further process development is, however, beyond the scope of this report.

In summary, our experimental results show that the light transmission of a polymer waveguide in a simple cladding/electrode geometry can be electrically controlled. In particular, over a device length of only about 200 µm close to unity signal modulation can be achieved. While

clearly the topics of material processing and required voltage range have to be further considered, the presented attenuator device demonstrates that miniaturized elastomer-based optical components might provide appealing alternatives to existing systems.

Acknowledgements Financial support by the Austrian Nano Initiative (Research Project Cluster 0700 Integrated Organic Sensors and Optoelectronics Technologies) and by the Austrian Federal Ministry for Transport, Innovation and Technology (BMVIT) is gratefully acknowledged.

References

1. J. Maher, R.L. Schank, G. Pfister, Appl. Phys. Lett. **29**, 293 (1976)
2. S. Uma, R. Matusiak, D.L. Hecht, E.J. Shrader, IEEE J. Sel. Top. Quantum Electron. **10**, 435 (2004)
3. S. Sakarya, G. Vdovin, P.M. Sarro, Sens. Actuators A **271**, 271 (2003)
4. M. Beck, R. Fiolka, A. Stemmer, Opt. Lett. **34**, 803 (2009)
5. M. Aschwanden, A. Stemmer, Opt. Lett. **31**, 2610 (2006)
6. N. Galler, H. Ditlbacher, B. Steinberger, A. Hohenau, M. Dansachmüller, F. Camacho-Gonzales, S. Bauer, J.R. Krenn, A. Leitner, F.R. Aussenegg, Appl. Phys. B **85**, 7 (2006)
7. C. Kluge, N. Galler, H. Ditlbacher, M. Gerken, Appl. Phys. A **102**, 407 (2011)
8. R. Pelrine, R. Kornbluh, Q. Pei, J. Joseph, Science **287**, 836 (2000)
9. G.B. Hocker, W.K. Burns, Appl. Opt. **16**, 113 (1977)
10. W. Karthe, R. Müller, *Integrierte Optik* (Akademische Verlagsgesellschaft Geest & Portig, Leipzig, 1991)